

Figure S1. Heatmap of I_R for CG methylation context in chromosomes 1, built for the 151 *Arabidopsis thaliana* ecotypes [14].

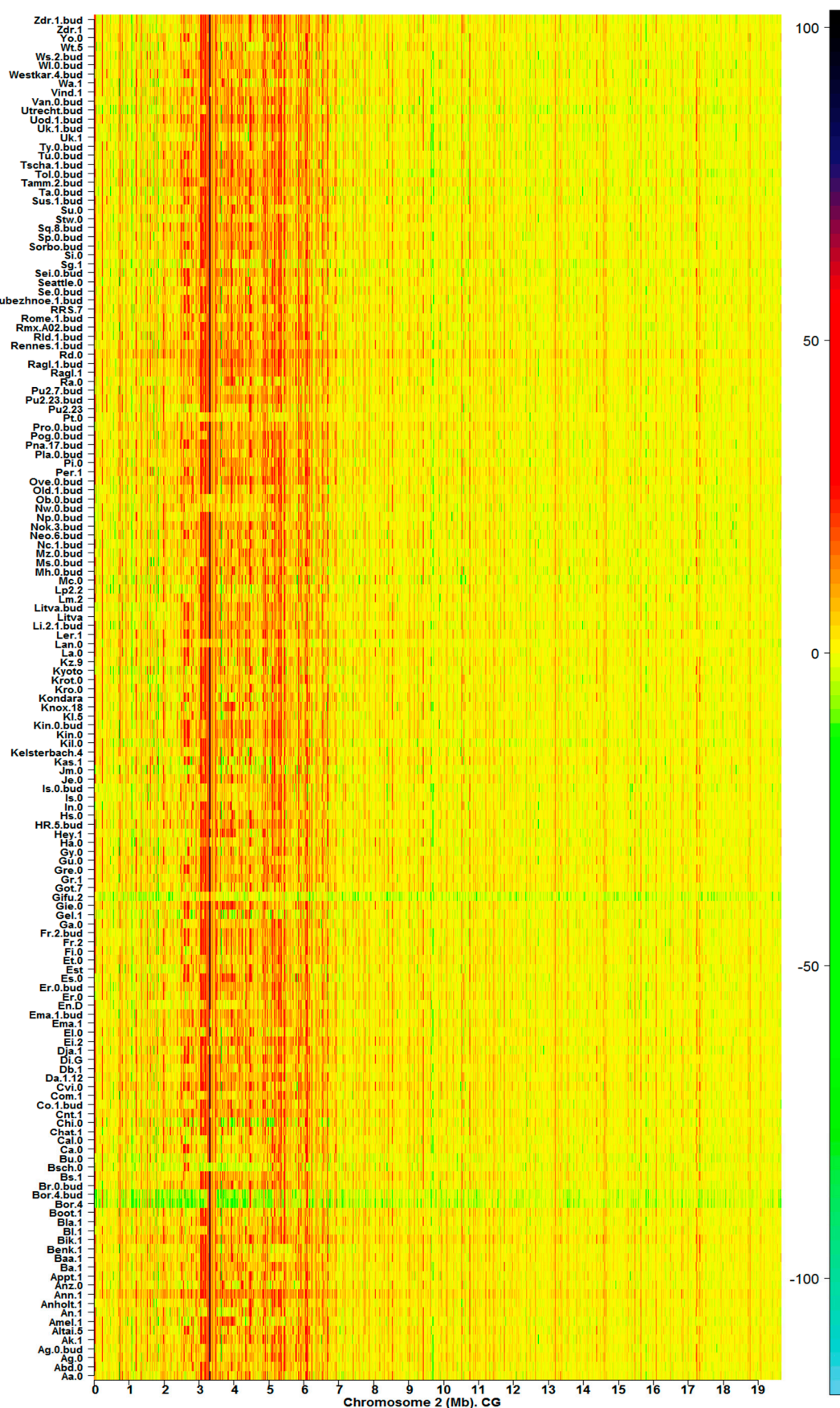


Figure S2. Heatmap of I_R for CG methylation context in chromosomes 2, built for the 151 *Arabidopsis thaliana* ecotypes [14]

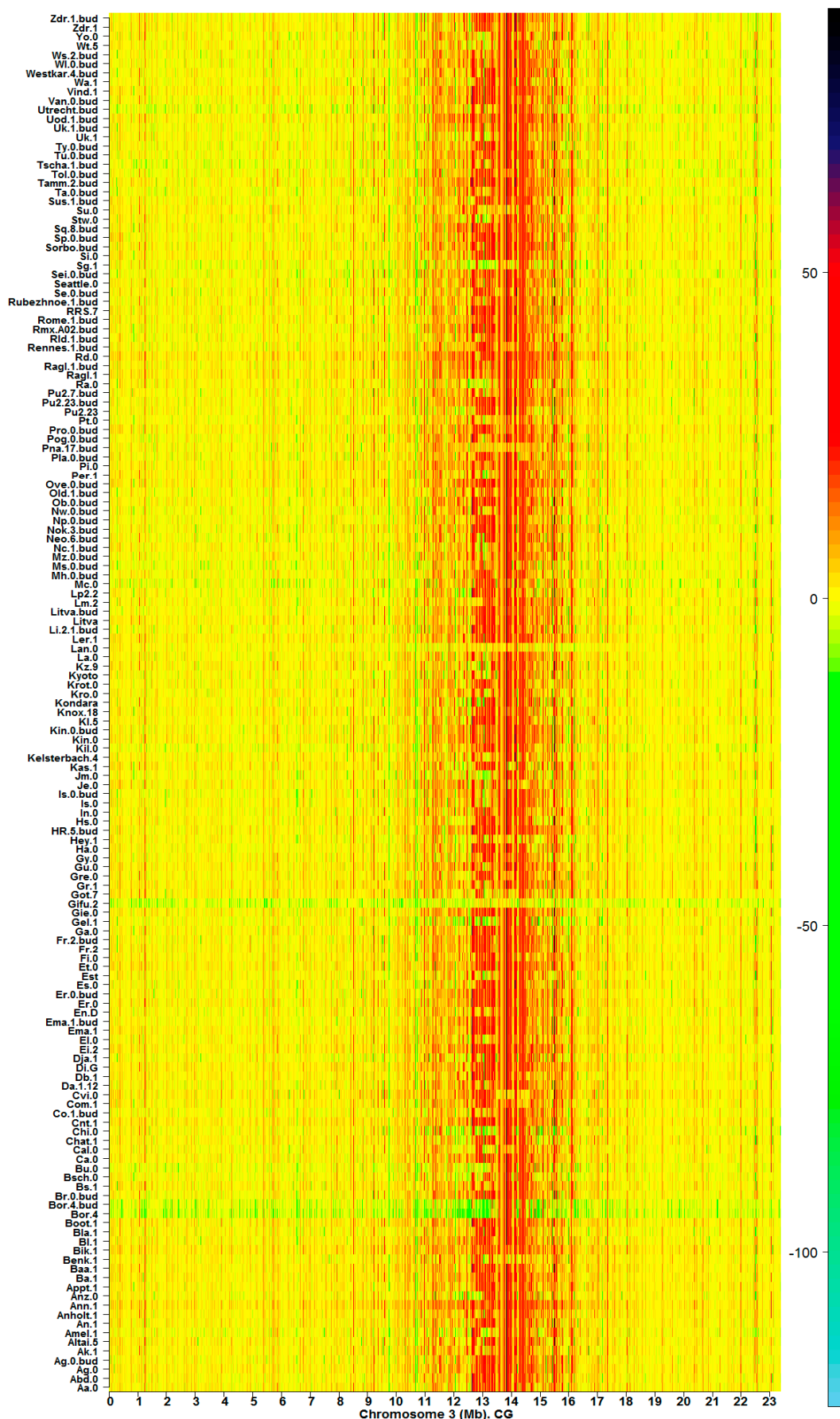


Figure S3. Heatmap of I_R for CG methylation context in chromosomes 3, built for the 151 *Arabidopsis thaliana* ecotypes [14]

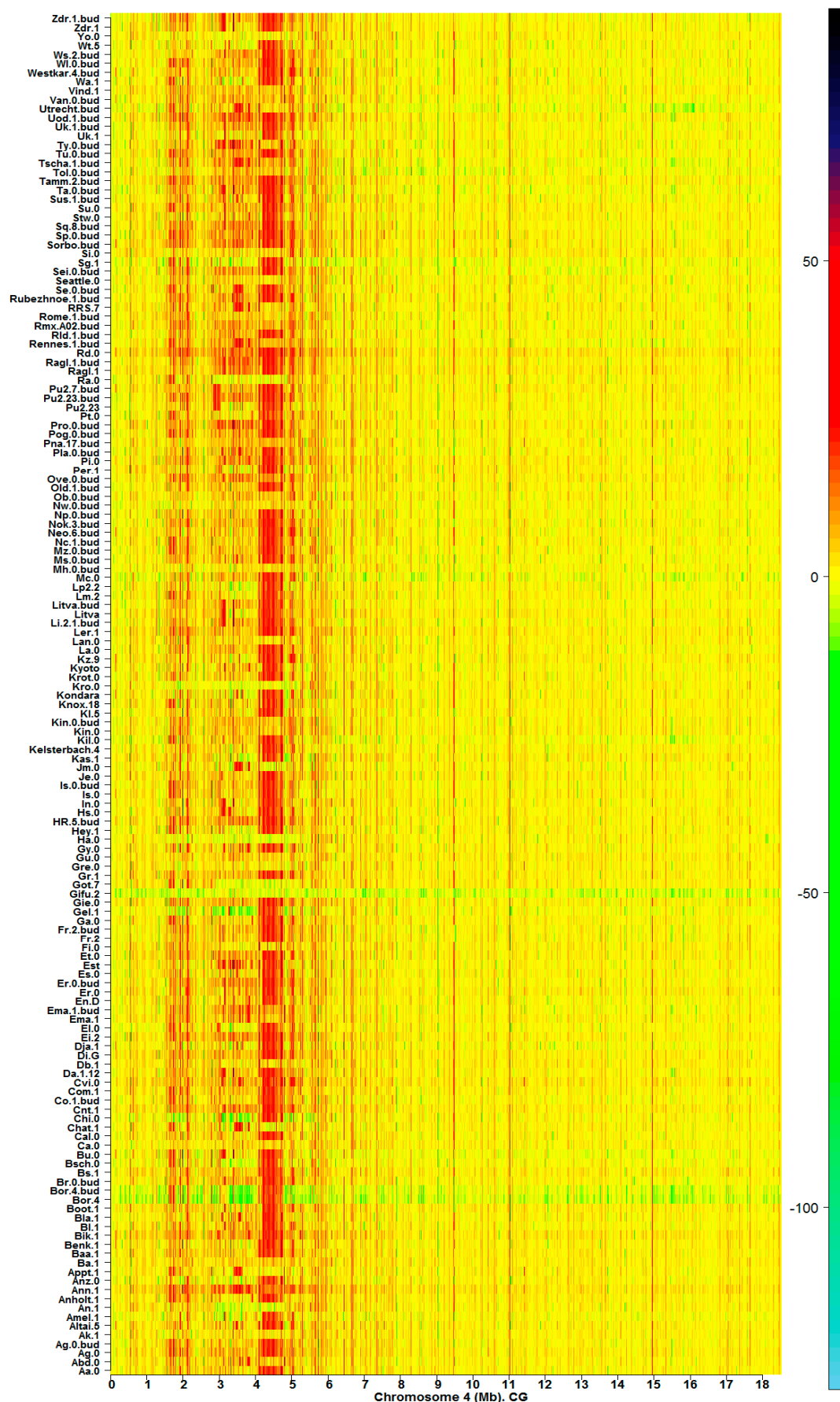


Figure S4. Heatmap of I_R for CG methylation context in chromosomes 4, built for the 151 *Arabidopsis thaliana* ecotypes [14]

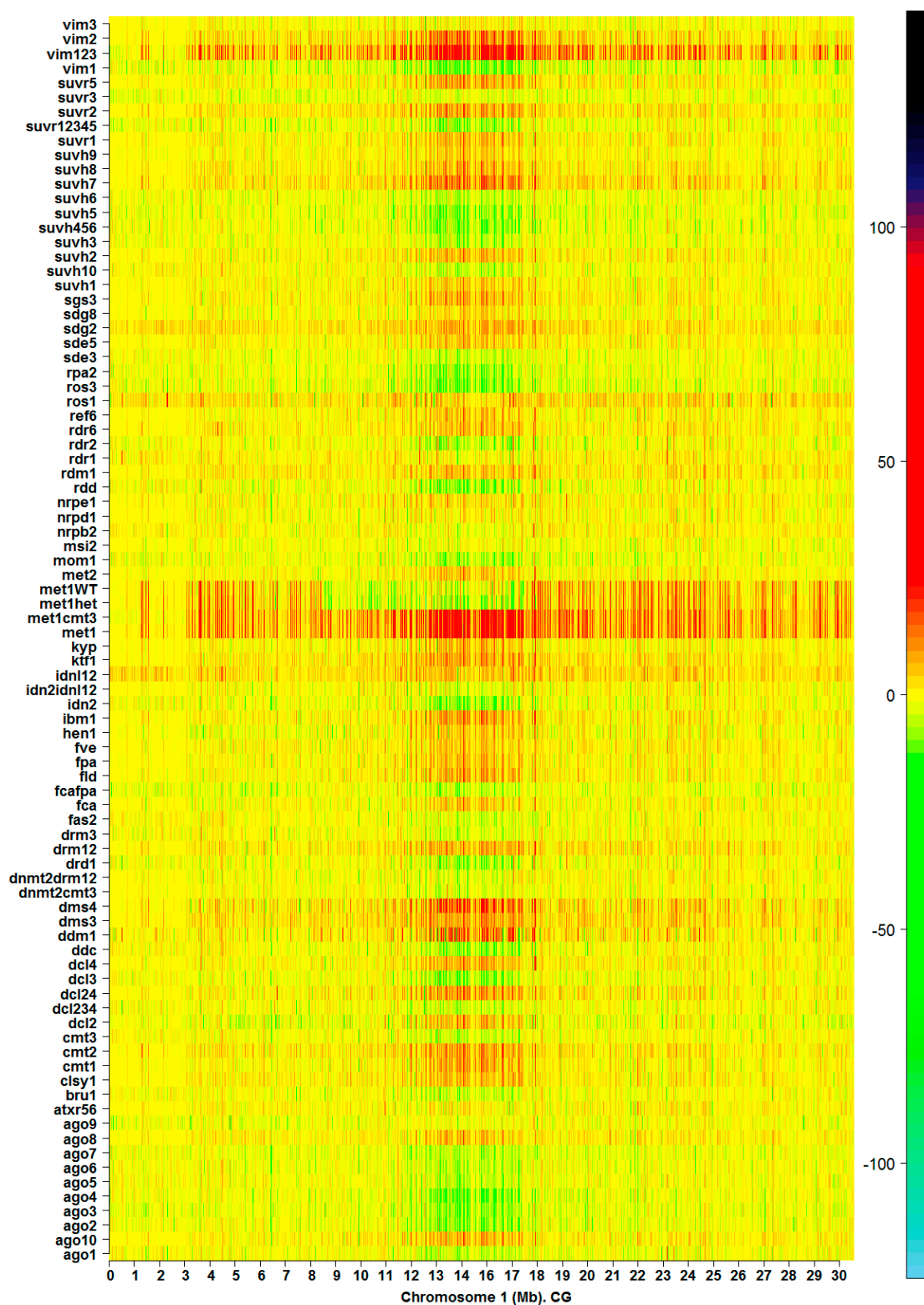


Figure S5. Heatmap of I_R for CG methylation context in chromosomes 1 built for 85 silencing mutants in *Arabidopsis thaliana* [15].

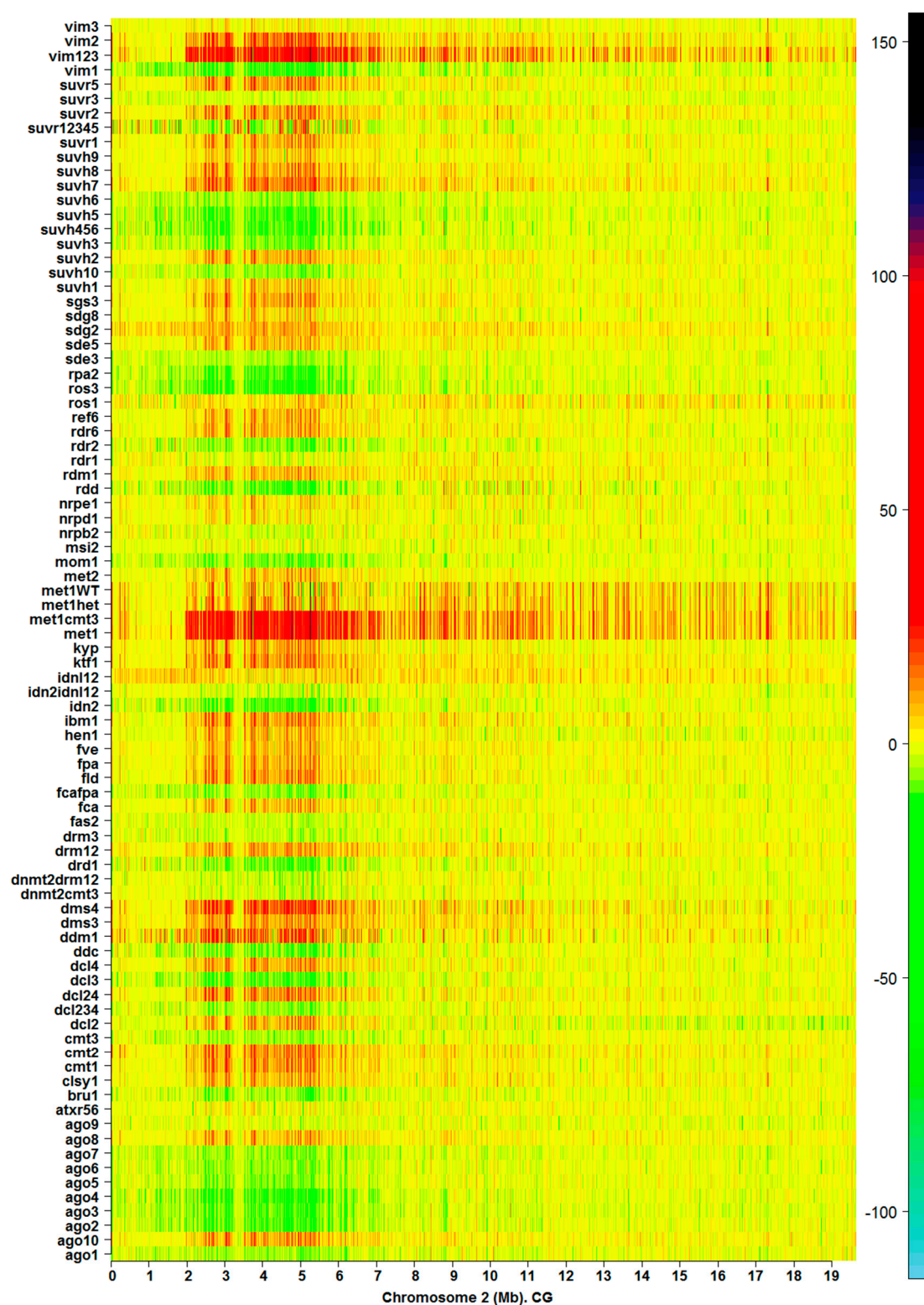


Figure S6. Heatmap of I_R for CG methylation context in chromosomes 2 built for 85 silencing mutants in *Arabidopsis thaliana* [15].

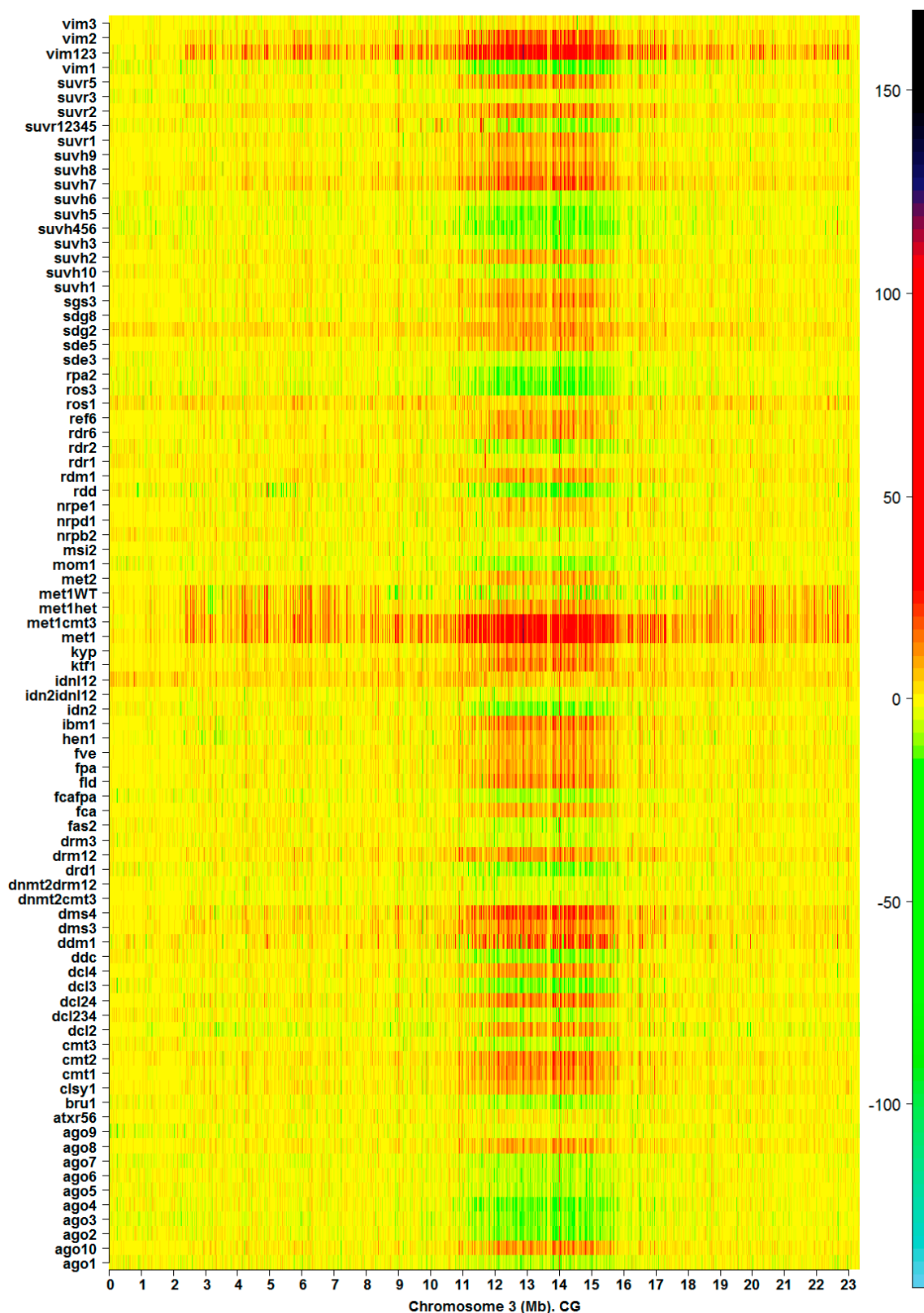


Figure S7. Heatmap of I_R for CG methylation context in chromosomes 3 built for 85 silencing mutants in *Arabidopsis thaliana* [15].

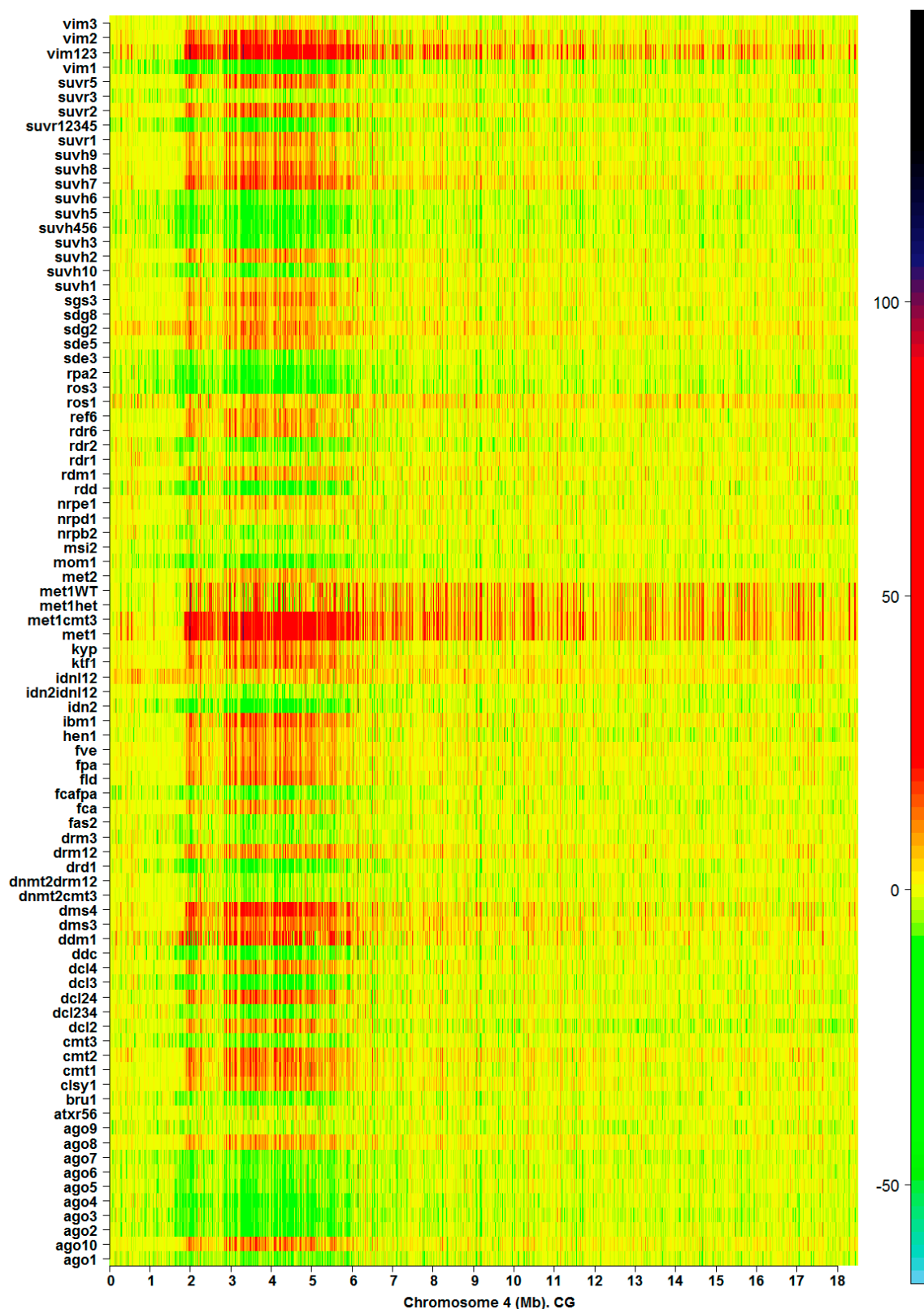


Figure S8. Heatmap of I_R for CG methylation context in chromosomes 4 built for 85 silencing mutants in *Arabidopsis thaliana* [15].

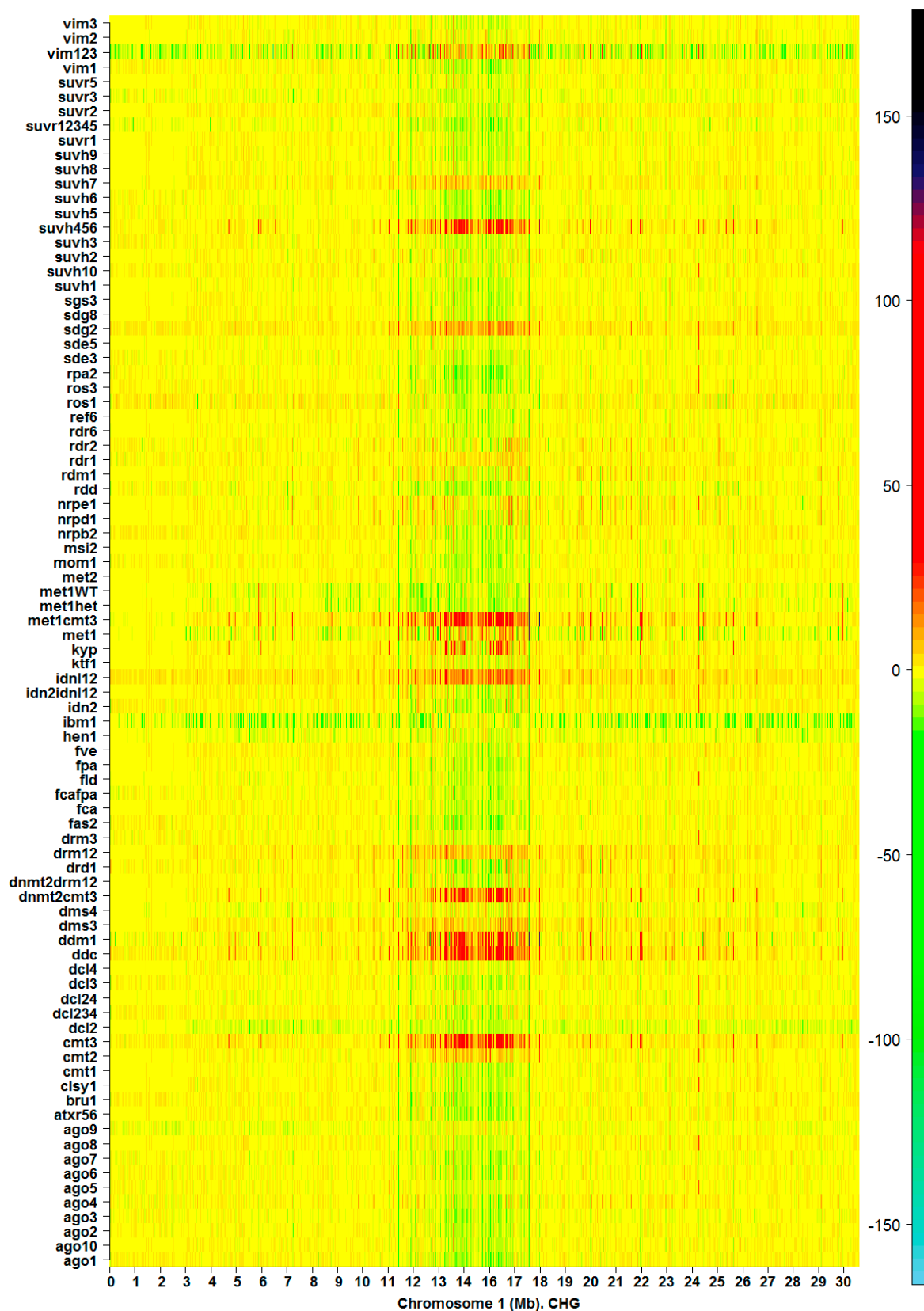


Figure S9. Heatmap of I_R for CHG methylation context in chromosome 1 built for the 85 silencing mutants [15].

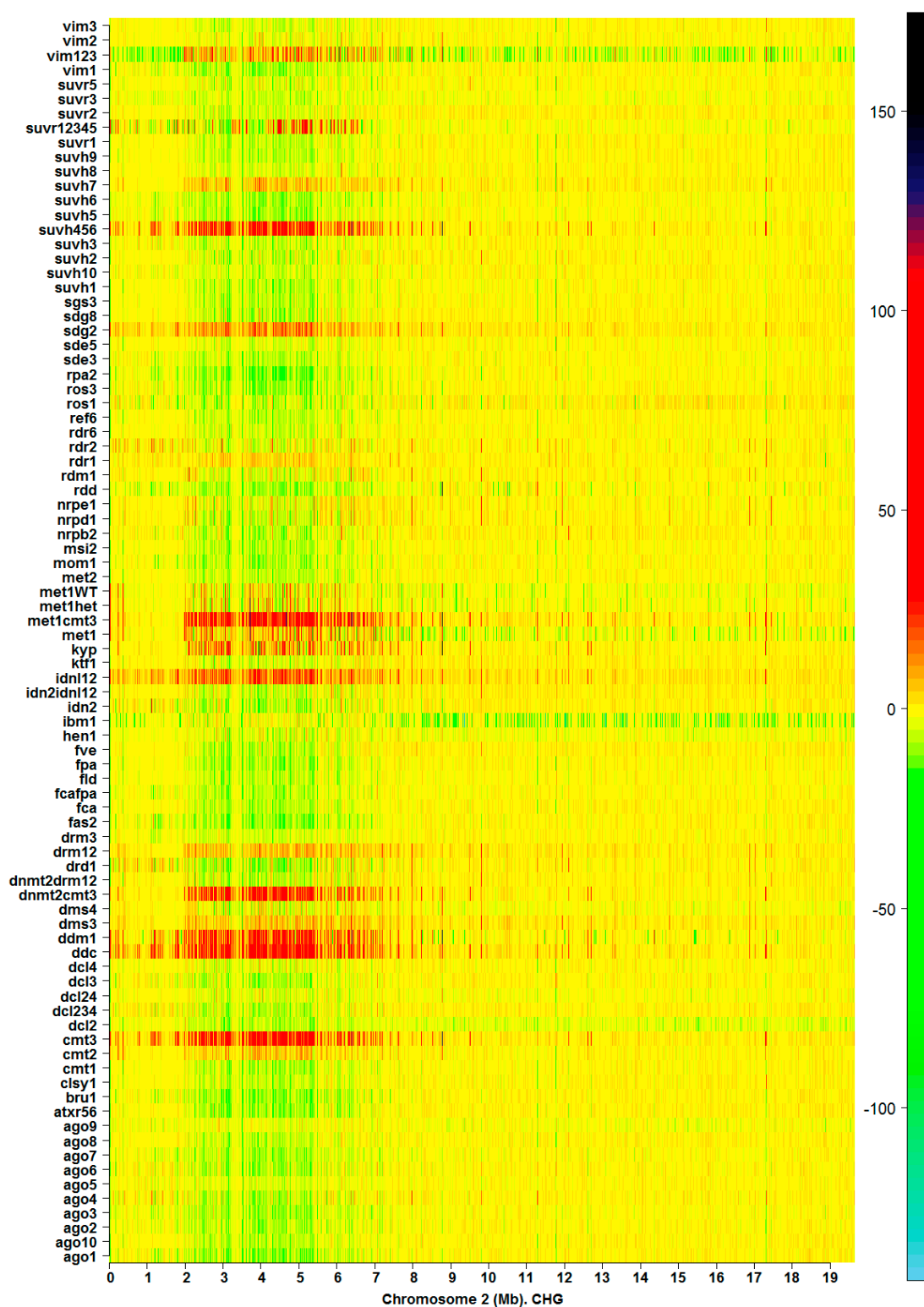


Figure S10. Heatmap of I_R for CHG methylation context in chromosome 2 built for the 85 silencing mutants [15].

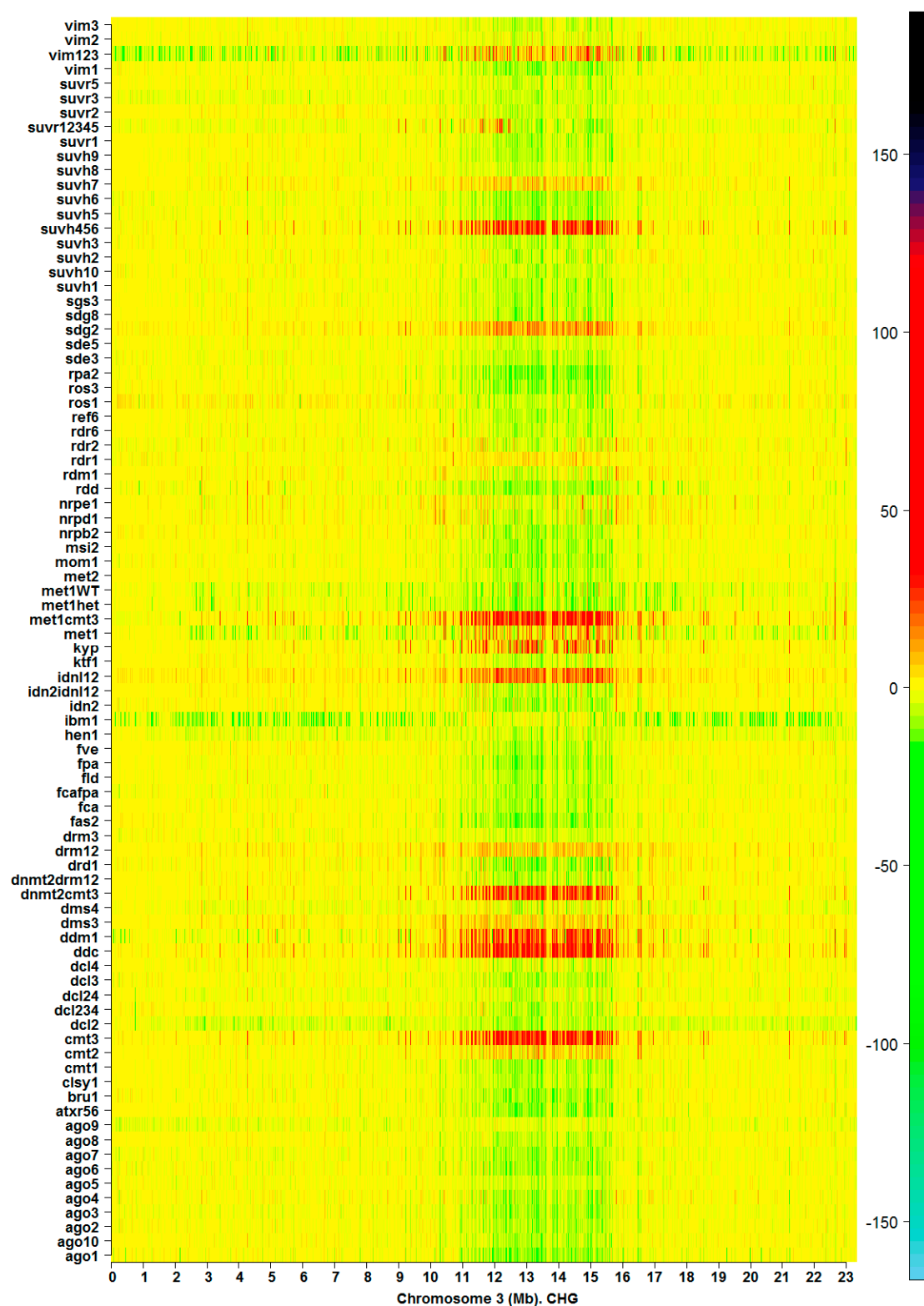


Figure S11. Heatmap of I_R for CHG methylation context in chromosome 3 built for the 85 silencing mutants [15].

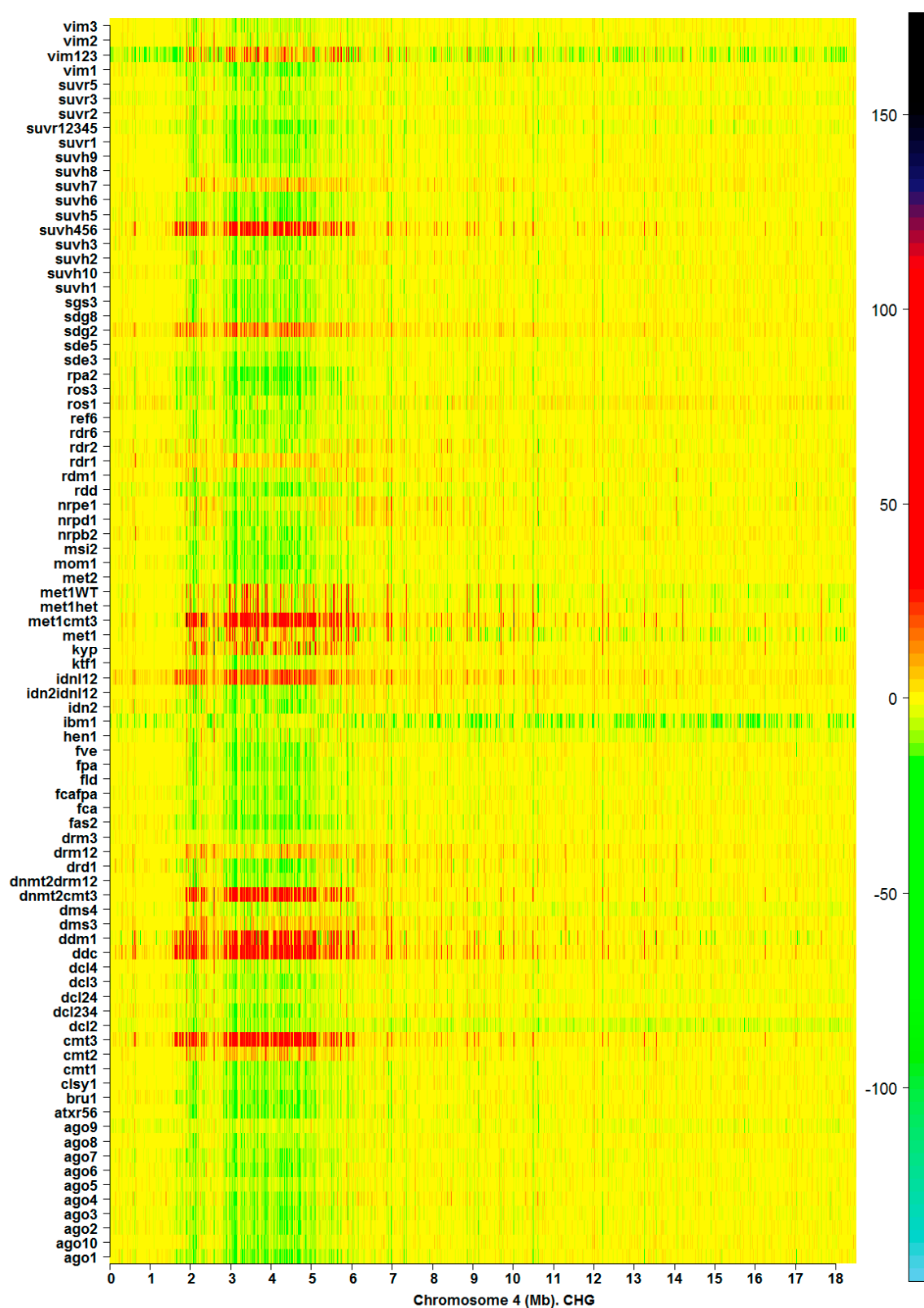


Figure S12. Heatmap of I_R for CHG methylation context in chromosome 4 built for the 85 silencing mutants [15].

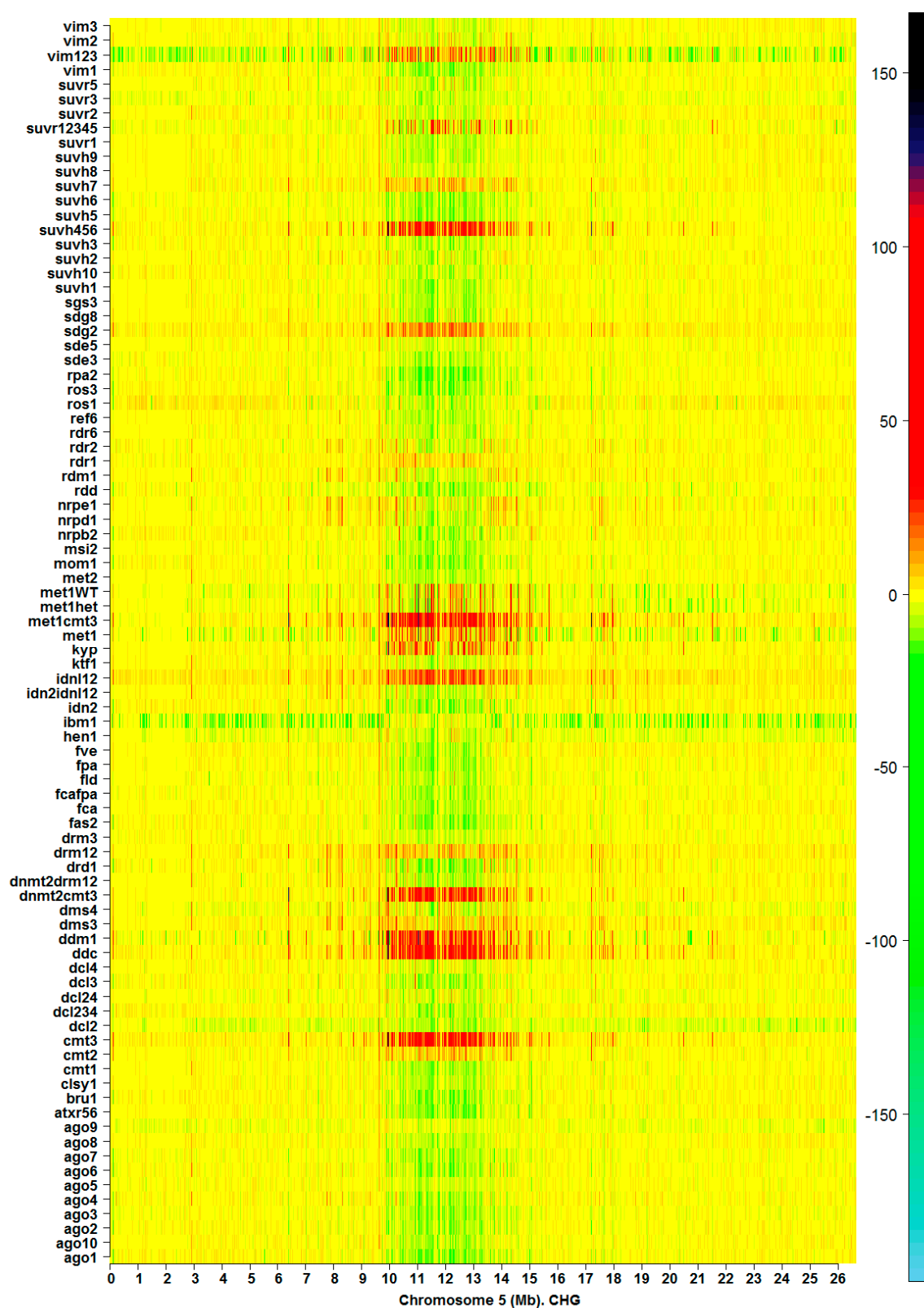


Figure S13. Heatmap of I_R for CHG methylation context in chromosome 5 built for the 85 silencing mutants [15].

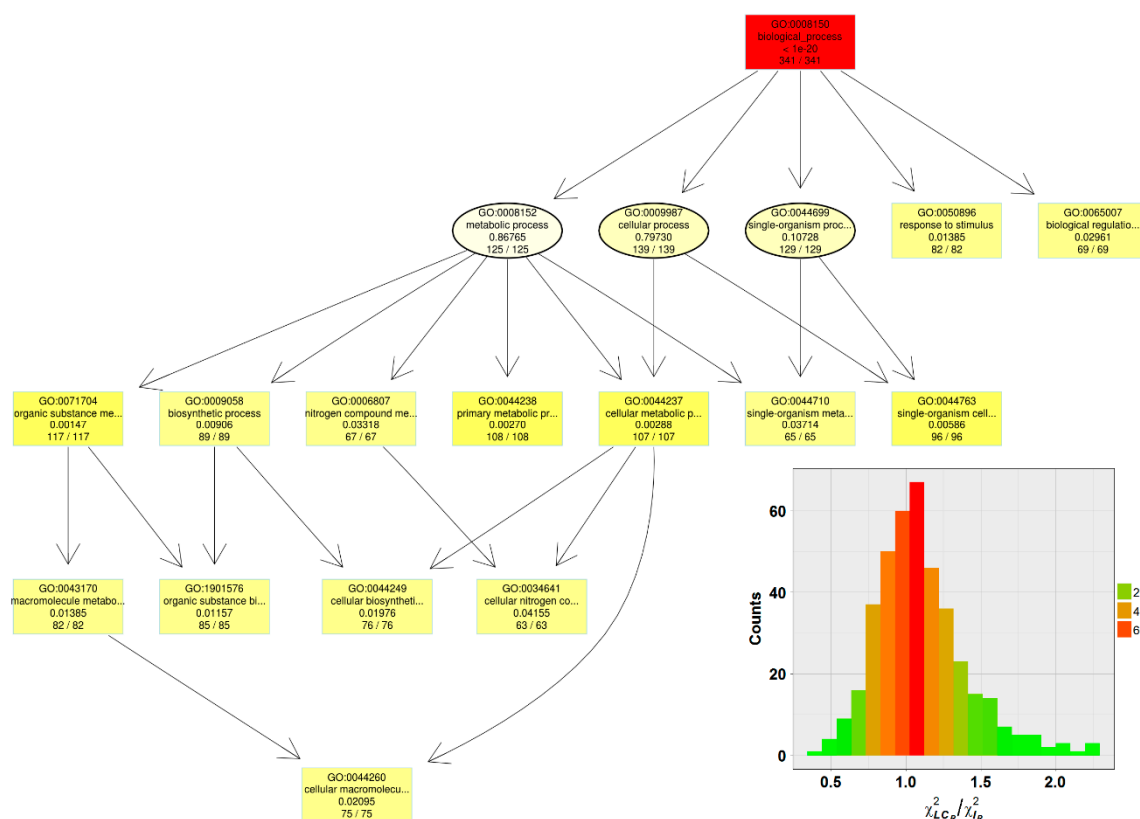


Figure S14. GO enrichment analysis of the genes within the selected GFs based on Chi-square statistics. The significant nodes are represented as rectangles and only the subgraph induced by the first 15 significant nodes is shown. The subplot shows the distribution of the rate $\chi^2_{LCR} / \chi^2_{IR}$ of the Chi-squared statistics estimated for GFs selected where the 477 annotated protein-code genes are located. The bootstrap Kolmogorov–Smirnov test does not reject normality rate $\chi^2_{LCR} / \chi^2_{IR}$ and a Student’s *t*-test indicates that the mean is significantly greater than 1 (although quantitatively not too much greater than 1, since the expected mean inferred for this population is around 1.1).

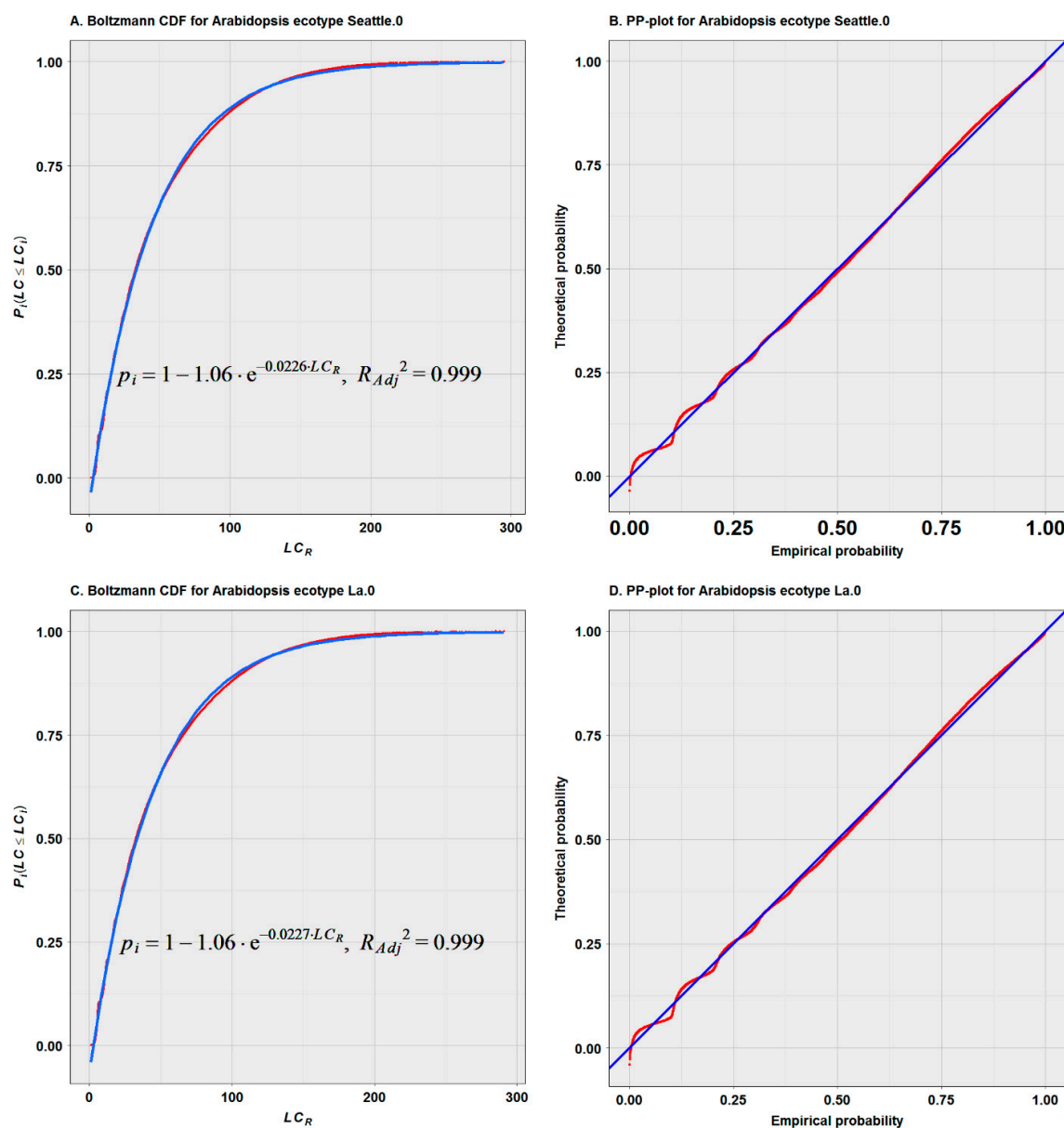


Figure S15. Non-linear regression fit of Equation (4) for *Arabidopsis* ecotypes Seattle.0 and La.0. (A); CDF and PP-plot *Arabidopsis* ecotype Seattle.0. (B,C); CDF and PP-plot *Arabidopsis* ecotype La.0. (D). In panels A and C, the blue and red lines denote the fitted and experimental probability values, respectively; In panels B and D, the red lines correspond to the graph: theoretical probability (y) versus empirical probability (x), and the blue lines are only the reference straight line $x = y$, which correspond to the ideal/perfect fit.

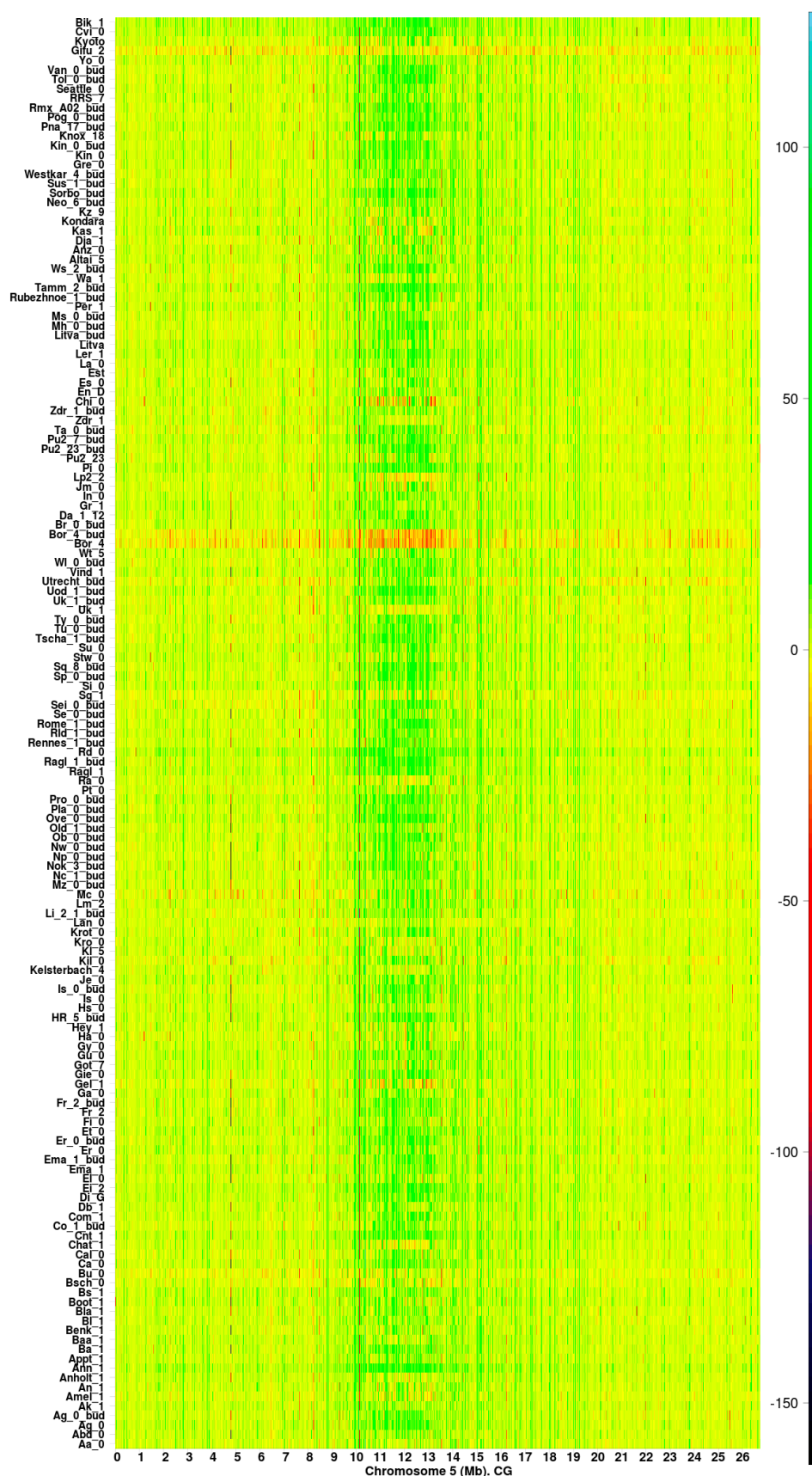


Figure S16. Heatmap for I_R in the CG methylation context along chromosome 5 from 151 *Arabidopsis thaliana* ecotypes. The samples are the same as in Figure 1, but with an inverted color scale equivalent to a photographic negative; the maximum and minimum correspond to sky blue and black, respectively.